

Collective flux creep: beyond the logarithmic solution

L. Burlachkov, D. Giller, and R. Prozorov

Institute of Superconductivity, Department of Physics, Bar-Ilan University,

Ramat-Gan 52900, Israel

(February 6, 1998)

Abstract

Numerical studies of the flux creep in superconductors show that the distribution of the magnetic field at any stage of the creep process can be well described by the condition of spatial constancy of the activation energy U independently on the particular dependence of U on the field B and current j . This results from a self-organization of the creep process in the undercritical state $j < j_c$ related to a strong non-linearity of the flux motion. Using the spatial constancy of U , one can find the field profiles $B(x)$, formulate a semi-analytical approach to the creep problem and generalize the logarithmic solution for flux creep, obtained for $U = U(j)$, to the case of essential dependence of U on B . This approach is useful for the analysis of dynamic formation of an anomalous magnetization curve ("fishtail"). We analyze the quality of the logarithmic and generalized logarithmic approximations and show that the latter predicts a maximum in the creep rate at short times, which has been observed experimentally. The vortex annihilation lines (or the sample edge for the case of remanent state relaxation), where $B = 0$, cause instabilities (flux-flow regions) and modify or even destroy the self-organization of flux creep in the whole sample.

PACs: 74.60.-w; 74.25.Ha; 74.60.Ec

Typeset using REVTeX

I. INTRODUCTION

Since the discovery of the giant vortex creep [1] in high-temperature superconductors (HTSC), it has become clear that the relaxation processes in these compounds may be very rapid compared to usual low-temperature superconductors. The magnetization current j and, in turn, the magnetic moment M , which is approximately proportional to j in most cases, drop considerably during the usual experimental time windows of a few hours (or even less) down to small values $j \ll j_c$, in particular, at elevated temperatures. Here j_c is the critical current, which divides the regimes of *flux creep* ($j < j_c$) characterized by the Boltzmann factor $\exp(-U/kT)$, where $U(B, j, T)$ is the activation energy for flux creep, and the non-activational *flux flow* ($j > j_c$) with $U = 0$. Due to such a pronounced relaxation, both j and M are determined in HTSC mostly by the flux dynamics in contrast with conventional superconductors where relaxation is usually very slow, so $j \cong j_c$ for any accessible time windows. This has given rise to an extensive study, both theoretical and experimental, of magnetic relaxation and vortex dynamics in HTSC (see [2–4] as reviews). Most of them are based on the logarithmic solution [5]:

$$U \simeq kT \ln \left(1 + \frac{t}{t_0} \right), \quad (1)$$

where t_0 is the logarithmic time scale for flux creep. We will discuss Eq. (1) in detail in Section III.

A closely related problem is the so-called "fishtail" effect, i.e., the anomalous increase of M as a function of H [6], or the increase of locally measured j as a function of B [7,8]. This effect serves as a test for different models of flux pinning and creep. The crucial question is whether the non-monotonous behavior of j results from the same feature in j_c ("static fishtail"), or arises from a faster relaxation of j at small B , whereas j_c is a monotonously decreasing function of B and itself shows no anomaly ("dynamic fishtail"). The latter possibility implies that the fishtail effect should disappear at shorter time windows or lower temperatures where the effect of relaxation is negligible and $j \cong j_c$ [9].

After the instantaneous switching on of the external field H , the flux-flow process develops towards establishing a nearly critical profile $j \cong j_c(B)$, where the Lorentz force $(j_c \times \phi_0)/c$ is compensated by the pinning force (ϕ_0 is the flux quantum and c is the velocity of light) all over the sample. Usually the duration τ_{flow} of flux flow does not exceed a few milliseconds (see Ref. [10] and references therein). As j drops below j_c , the slow process of flux creep starts. The creep rate is mostly determined by the Boltzmann factor $\exp(-U/kT)$, where $U = U(B, j)$. Of course, U depends also on temperature, but the creep experiments are usually conducted at constant temperature. In many cases the dependence of U on B can be neglected, which implies a crucial simplification for the theoretical description of flux creep. For instance, in an infinite slab of width $2d$ ($-d < x < d$) in the parallel external field H , the variation of the magnetic induction $\delta B = B(d) - B(0)$ do not exceed H^* , where $H^* = (4\pi/c)j_c d$ is the full penetration field [11] (j_c is considered to be field-independent). For $H \gg H^*$ one can neglect $\delta B \lesssim H^*$. If both j_c and d are sufficiently small, say, $j_c \simeq 10^4$ A/cm² and $d \simeq 0.1$ mm, then H^* is of order hundreds of Gauss. In this case the above condition is easily fulfilled for most H , and the activation energy appears to be field-independent: $U(j, B) \cong U(j, H)$. Then the field profiles $B(x)$ are almost straight [10,12], i.e., $j \cong const$ throughout the sample at all creep stages.

However, in larger samples ($d \gtrsim 1$ mm) with strong pinning ($j_c > 10^5$ A/cm²), one gets $\delta B \simeq H^* > 1$ Tesla, which implies that the spatial variation of B may not be small compared to H . Of course this estimation may not be valid at high temperatures where j_c drops. But for large and not too clean samples well below T_c the dependence of U on B is essential, and the field profiles are not straight. On the other hand, due to very fast relaxation B can vary by orders of magnitude during experimental time windows of order of hours (see, for instance, [7]), which also requires taking the $U(B)$ -dependence into account for the consistent description of the relaxation process, especially in the dynamic models of the fishtail formation.

The goal of this paper is to study the relaxation process for various dependencies of U on j and B . In Section II we show that the field profile at any stage of the relaxation process

can be described by the condition of spatial constancy of the activation energy:

$$U(x) \cong \text{const} \tag{2}$$

throughout the whole sample, where *const* depends on time only. Since $U = U(B, j)$, Eq. (2) provides an implicit relationship between B and j , manifesting a condition of *self-organization* of flux motion in the undercritical regime $j < j_c$. In other words, according to Eq. (2) the field profiles form a one-parameter family $B_U(x)$. The problem to be solved in order to describe the flux creep is to find these profiles together with the dependence of U on time. Note that this case differs from the self-organized criticality (see the pioneering work [13] and further applications to the superconductors in a critical state [14]), where the peculiarities of the flux motion (avalanches, critical exponents, etc.) are considered in the vicinity of the critical state $j \cong j_c$ (i.e., at $U \cong 0$). The condition $j \cong \text{const}$ found in previous studies [10,12] is obviously just a particular case of Eq. (2) provided U is independent of B . In Section III we analyze numerically and, using Eq. (2), semi-analytically the flux creep for various $U(B, j)$ -dependencies, particularly for the most general collective creep behavior $U \propto B^\alpha j^{-\mu}$. We show that at short, but experimentally available time scales the creep process differs significantly from the logarithmic solution (see Eq. (1)) and shows a maximum in the relaxation rate, $dU/d \ln t$, in accordance with the experimental data. The semi-analytical solution provides a good approximation to the exact (numerical) one at all time scales. In Section IV we apply these ideas to the problem of the anomalous magnetization curve (fishtail) and show how the dynamic development of the anomaly in j (or the same, in $M \propto j$) can be described semi-analytically. In Section V we study the effect of so-called "annihilation lines" in infinitely long samples, where B changes sign and vortices with opposite directions annihilate each other, on the self-organization of the flux motion. A particular case of such a line is the edge of the infinitely long sample in the remanent state. The vortex velocity v shows a peculiarity (divergence) at such a line, resulting in the appearance of flux-flow regions in the vicinity of the annihilation lines. We show that these peculiarities affect deeply the self-organization of creep and the condition of spatial

constancy for U (see Eq. (2)) is modified or even destroyed in the whole sample (and not only in the vicinity of the annihilation lines).

II. SPATIAL CONSTANCY OF U

Consider an infinite slab of thickness $2d$ ($-d < x < d$) with the magnetic field $B(x)$ parallel to z -direction and the current j flowing along y . The external field H is switched on instantaneously when no vortices are present in the sample, which corresponds to zero-field-cooled experiments. We consider $H \gg H_{c1}$, where H_{c1} is the lower critical field, and disregard the effects related to the latter.

The flux creep is described by the diffusion equation [15]:

$$\frac{\partial B}{\partial t} = -\frac{\partial D}{\partial x}, \quad (3)$$

where

$$D = Bv = \mathcal{A} \frac{\phi_0}{c\eta} B j \exp(-U/kT) \quad (4)$$

is the magnetic flux current, v is the vortex velocity, η is the Bardeen-Stephen drag (friction) coefficient [16] for flux flow and \mathcal{A} is a numerical factor. Note that D is proportional to the electric field $E = (B \times v)/c$ in the sample. The form of the magnetic flux current D is chosen such that at $U = 0$ and $\mathcal{A} = 1$ the flux velocity v corresponds to the Bardeen-Stephen expression [16] for the flux flow: $v = v_{flow} = \phi_0 j / c\eta$.

It has been already discussed [2] that the strongly non-linear Eq. (3) should obey a self-organized behavior. This means that if a fluctuation δU appears in the sample, it results in a significant (exponential) local change of the flux current $D \propto \exp(-\delta U/kT)$ which, in turn, leads to fast smearing out of the fluctuation. In other words, $|\delta U| \simeq kT$ is the scale of "permitted" variations of U . This has been proved experimentally by direct measurements of U using the Hall probe technique [17]. We suggest a more general criterion of self-organization as follows.

The variation of the flux current density D (or the same, of the electric field E) within the sample can be written as:

$$\delta D = \frac{\partial D}{\partial B} \delta B + \frac{\partial D}{\partial j} \delta j + \frac{\partial D}{\partial U} \delta U, \quad (5)$$

where B , j and U are formally considered as three relaxing parameters, though $U = U(B, j)$. If one of the three terms in the right-hand-side of Eq. (5) appears to be considerably greater by absolute value than the other two terms, the corresponding parameter governs the relaxation process, i.e., relaxes towards its mean value irrespective of what happens with the other two. Obviously, this leads to a self-organization of the flux diffusion process which implies that the three terms in the right-hand-side of Eq. (5) tend to keep the same order:

$$\frac{\partial D}{\partial B} \delta B \cong \frac{\partial D}{\partial j} \delta j \cong \frac{\partial D}{\partial U} \delta U. \quad (6)$$

The above condition can be considered as a mutual confinement for variations of B , j and U . Taking the expression for D from Eq. (4), we get a limitation for δU :

$$\frac{\delta U}{kT} \lesssim \max \left\{ \frac{\delta B}{B}, \frac{\delta j}{j} \right\}. \quad (7)$$

Note that the above estimation does not require the condition $U \gg kT$, i.e., it should hold starting from the very early stages of flux creep.

If one of the three terms in Eq. (6) is very small (or absent) for any "external" reason, then the self-organization applies to the two other ones. For instance, if B is much greater than H^* and thus $\delta B/B \ll 1$, we get:

$$\frac{\delta U}{kT} \simeq \frac{\partial U}{\partial j} \frac{\delta j}{kT} \simeq \frac{U_c}{kT} \frac{\delta j}{j_c} < 1, \quad (8)$$

where U_c is the characteristic activation energy for $j \rightarrow 0$. Since in general $U_c \gg kT$, we get $\delta j < (kT/U_c) j_c \ll j_c$, as has already been discussed in Ref. [10].

It is worth mentioning, however, that at the locations where $j = 0$ or $B = 0$ the variations of U can exceed kT significantly, as follows from Eq. (7). The first of these two conditions ($j = 0$) regularly holds at the center of the sample, and we will comment on this point in

the following Section III. The second condition ($B = 0$) holds at the lines where vortices of different sign annihilate each other, or just at the edge of the sample in the remanent state. We will devote special Section V for the latter case.

Eqs. (7)-(8) prove the spatial constancy of U throughout the sample with a kT precision (see Eq. (2)). The analytical results based on Eq. (2) we will refer below as "semi-analytical" ones.

III. ONE-DIMENSIONAL CREEP EQUATION

In an infinite slab the current j is related to B by the Maxwell law:

$$j = -\frac{c}{4\pi} \frac{\partial B}{\partial x}, \quad (9)$$

if one uses a reference system xyz where $B \parallel z$ and $j \parallel y$. For a platelet sample in a perpendicular external field, where the in-plane field component B_x appears, the relation between j and B becomes more complicated [4,18]. Here we focus on the one-dimensional creep problem where $B_x = 0$, so $B_z = B$.

After substituting Eq. (9) into Eq. (3) one gets the basic one-dimensional equation for flux motion:

$$\frac{\partial B}{\partial t} = \frac{\partial}{\partial x} \left(\mathcal{A} \frac{\phi_0}{4\pi\eta} B \frac{\partial B}{\partial x} \exp(-U/kT) \right). \quad (10)$$

The numerical coefficient \mathcal{A} depends on the creep mechanism and should not necessarily be of order of unity [19] (see also discussion in Ref. [10]). However, the low field measurements (i.e., in the single vortex pinning regime) in $\text{YBa}_2\text{Cu}_3\text{O}_{7-x}$ crystals [17], where Eq. (10) was experimentally studied by direct local measurements of B , $\partial B/\partial x$ and $\partial B/\partial t$, revealed that $\mathcal{A} \simeq 1$. Thus, at least in the case of single vortex pinning, Eq. (10) is consistent with the equation for flux flow:

$$\frac{\partial B}{\partial t} = \frac{\partial}{\partial x} \left(\frac{\phi_0}{4\pi\eta} B \frac{\partial B}{\partial x} \right), \quad (11)$$

since the latter can be obtained from Eq. (10) at $U = 0$ and $\mathcal{A} = 1$.

The features of self-organized criticality in the solution of Eq. (10) have been analyzed [20] for the case of switching on of a small additional field δB on the background of $B \gg \delta B$ already present in the sample, and for a specific (logarithmic) dependence of the activation energy on the current: $U = U_0 \ln(j_0/j)$. In terms of the energy distribution $U(x)$ across the sample the case considered in Ref. [20] implies that in the beginning the energy was very large (or infinite) in the whole sample, since $j = 0$, then an area of small U appeared at the edge (after switching on δB), and the propagation of this "fluctuation" of the $U(x)$ profile was studied.

In contrast with Ref. [20] we consider below the instantaneous switching on or removal of the whole external field H . A sort of self-organization, i.e., establishing of a "partial critical state" [21] with $j(B) \propto j_c(B)$ has already been reported for this case. We show below that this result follows from our more general approach based on Eq. (2) if $U = U(j/j_c(B))$, but for an arbitrary $U(B, j)$ -dependence the partial critical state may not be established. Our general results on self-organization of the flux creep do not depend on the specific $U(B, j)$ -dependence, but focus on the collective creep behavior $U(B, j) \propto B^\alpha j^{-\mu}$ as mostly relevant in HTSC. We will not consider the time-dependent boundary conditions $H = H(t)$. Some results for the latter case can be found in Refs. [22,23].

The integration of Eq. (10) can be performed as follows. Defining the magnetization as:

$$m = \frac{1}{2d} \int_{-d}^d (B - H) dx \quad (12)$$

and integrating Eq. (10) over x , we get:

$$\frac{\partial m}{\partial t} = \mathcal{A} \frac{\phi_0}{4\pi\eta d} H \left| \frac{\partial B}{\partial x} \right|_{x=\pm d} \exp(-U_{edge}/kT), \quad (13)$$

where $U_{edge} = U(x = \pm d)$ is the activation energy at the edges of the slab. For the case (discussed below) of straight field profiles: $|\partial B/\partial x| \cong const$, and constancy of the activation energy (the latter implies that U_{edge} can be substituted by the mean and almost constant U over the sample, see Eq. (8)), one can rewrite Eq. (13) in the form:

$$\frac{\partial m}{\partial t} \cong \mathcal{A} \frac{m}{\tau} \exp(-U/kT), \quad (14)$$

where $\tau = 2\pi\eta d^2/\phi_0 H$.

A. Flux flow ($j > j_c$)

After switching on the external field H , the flux flow starts and lasts until the vortices fill the sample up to the critical profile j_c . Its duration τ_{flow} can be easily estimated if one notices that already during the flow regime the $B(x)$ -profiles are almost straight, i.e., $|j| = (c/4\pi) |\partial B/\partial x| \simeq const$ (see dashed lines in Fig. 1a). Using the straightness of the field profiles, one can estimate the magnetization m as:

$$m(j) \cong H - \frac{cH^2}{8\pi jd} \quad \text{for } j > j^*, \quad (15)$$

$$m(j) \cong \frac{2\pi jd}{c} \quad \text{for } j < j^*, \quad (16)$$

where the current $j^* = cH/4\pi d$ shown as a grey solid line in Fig. 1a discriminates between the incomplete and complete penetration of flux into the sample. Note that we have chosen $H > H^*$, where $H^* = 4\pi j_c d/c$ is the field of full penetration. This means that $j_c < j^*$, i.e., by the completion of the flux flow stage, flux penetrates the whole sample (see Fig. 1a). Then, substituting these values into Eq. (13) and solving it at $U = 0$ and $\mathcal{A} = 1$, we get:

$$j \cong j^* \sqrt{\frac{\tau}{2t}}, \quad t < \tau/2 \quad (17)$$

$$j \cong j^* \exp\left(\frac{1}{2} - \frac{t}{\tau}\right), \quad t > \tau/2 \quad (18)$$

where $\tau/2 = \pi\eta d^2/\phi_0 H$ is the time of full penetration in the flux flow regime. For $j_c < j^*$ the time of establishing of the critical profile after switching on the external field is $\tau_{flow} \equiv t(j_c) = (\tau/2)(1 + 2 \ln j^*/j_c) \simeq \tau$ as follows from Eq. (18).

The crossover from the flux flow to flux creep process is well defined, i.e., the critical profile $j = j_c$ is established at $t = \tau_{flow}$ almost exactly throughout the whole sample (see Fig. 1a). More exactly, the fluctuations of U which appear in the whole slab at the crossover from flow to creep ($j \cong j_c$) are of order kT according to Eq. (8), therefore $\delta j < (kT/U_c)j_c \ll j_c$. The only exclusion is the very center of the slab, $x \cong 0$, where $j = 0$ and U shows

relatively strong variations, as we discussed in the previous Section. However, this area is narrow and can be neglected when considering the profiles $B(x)$ and magnetization m .

After the flux flow stage is completed, a much slower process of flux creep starts, and various cases of $U(B, j)$ can be analyzed. First we consider the simplest case where U depends only on j .

B. Creep at $j_c = \text{const}$, $U = U(j)$

This case has been already studied in Refs. [10,12,21,24]. Here we analyze it as a test for our numerical solution before consideration of more complicate models of $U(B, j)$. During the stage of flux creep ($j < j_c$) (see Fig. 1a), the field profiles are even more straight than during the flux flow stage [10,12], i.e., $|j| \cong \text{const}$, and, in turn, $U(j) \cong \text{const}$ (see Fig. 1b). Note a very narrow increase of δU at $x = 0$, where $j = 0$, which is consistent with the comment at the end of Section II.

Since U_{edge} is approximately equal to the mean U over the sample, one gets from Eqs. (13) and (16), using also Eq. (9):

$$\frac{dU}{dt} = \frac{dU}{dj} \frac{dj}{dm} \frac{dm}{dt} \cong \frac{\mathcal{A}}{\tau} j \left| \frac{dU}{dj} \right| \exp(-U/kT). \quad (19)$$

This equation can be integrated numerically for any $U(j)$ -dependence, and also can be solved with a logarithmic accuracy [5], see Eq. (1). The latter means that the real $U(j)$ -dependence is substituted by the tangent straight line with a slope dU/dj , as shown in Fig. 2, which is reasonable since the relaxation slows down exponentially as U grows. Thus the system spends most of the relaxation time near the final point where $U(j)$ and its tangent line almost coincide. Such an approximate solution of Eq. (19) acquires the form of Eq. (1) with

$$t_0 = \frac{kT}{|dU/dj|} \frac{2\pi\eta d^2}{\mathcal{A}\phi_0 j H} = \frac{\tau kT}{\mathcal{A} j |dU/dj|}. \quad (20)$$

As becomes clear from Eq. (1) and Fig. 2, t_0 is the time required to get from $U = -\infty$ (which corresponds to $t = -t_0$) to $U = 0$ (which corresponds to $t = 0$) along the non-physical part

of the tangent line, corresponding to negative U . Thus t_0 has no direct physical meaning and should not be mixed with the characteristic duration $\tau_{flow} \simeq \tau$ of flux flow, see Eqs. (17)-(18).

Eqs. (1) and (20) provide a logarithmic approximation for the time required for a system to reach the energy U . However, in order to use Eq. (1) to describe the $U(t)$ -dependence one observes that t_0 is not actually a constant and depends on U (or the same, on t). This effect is not of great importance at $dU/dj \simeq const$, i.e., where U is an almost linear function of j , but cannot be neglected in the opposite case of strongly non-linear dependence of U on j , where dU/dj changes significantly.

Consider the case of the collective creep model

$$U = U_c [(j_c/j)^\mu - 1], \quad (21)$$

which is an example of such a non-linear dependence. Here the exponent μ varies [2] from $\mu = 1/7$ (single vortex creep) to $\mu = 5/2$ (small bundles). The straightforward solution of Eq. (19) then gives:

$$\text{Ei} \left(\frac{U_c + U}{kT} \right) - \text{Ei} \left(\frac{U_c}{kT} \right) = \mathcal{A}\mu \frac{t}{\tau} \exp \left(\frac{U_c}{kT} \right), \quad (22)$$

where Ei is the integral exponential function. The logarithmic approximation for Eq. (22) acquires the form:

$$U = kT \ln \left(1 + \mathcal{A}\mu \frac{t}{\tau} (U + U_c)/kT \right), \quad (23)$$

which, if compared with Eq. (1), implies:

$$t_0 = \frac{\tau kT}{\mathcal{A}\mu(U + U_c)}. \quad (24)$$

If during the creep process j decreases down to $j_{\min} \ll j_c$, then the energy increases up to $U_{\max} \gg U_c$, where $U_{\max} = U(j_{\min})$, and t_0 decreases down to $t_0^{\min} \cong \tau kT / \mathcal{A}\mu U_{\max}$. Regularly, the latter estimation, $t_0 \cong t_0^{\min}$, is substituted into the logarithmic solution Eq. (1), and time dependence of t_0 is neglected. This results in an almost linear dependence of U on $\ln(t)$ (see Fig. 3). Let us call such an approximation (where t_0 is treated as a constant) as a "pure" logarithmic solution, whereas Eqs. (23)-(24) provide a "generalized" one.

The straightforward solution and both generalized and pure logarithmic ones are compared in Fig. 3. In the same figure we show an exact numerical solution of Eq. (10) obtained without any assumptions on spatial constancy of U . We used $\tau/\mathcal{A}\mu$ as a useful time constant in Fig. 3. One observes that the generalized logarithmic solution works at all t , and together with the straightforward solution provide a perfect fit to the exact one. On the other side, the pure logarithmic solution shows significant deviations from the exact one, especially at short times. This is consistent with Eq. (24), since there $U \lesssim U_c$, and, in turn, $t_0 \gg t_0^{\min}$. Particularly, the logarithmic solution misses the characteristic maximum in the creep rate $dU/d\ln t$ which appears at $\mathcal{A}\mu t/\tau \cong 10$. For $\eta \simeq 10^{-5}$ g/cm·sec [25] (which implies that T is well below T_c), $\mathcal{A} \simeq 1$, $\mu = 1/7$ (single vortex creep) and $d = 1$ mm, the maximum in $dU/d\ln t$ appears at $t^* \simeq 60/H$ sec, where H is measured in Oe. Thus the maximum or at least its tail can be resolved at experimentally accessible times. Note that the numerical factor in the latter estimation grows $\propto d^2$, and for some larger samples t^* can be significantly greater. The position of such a maximum determined experimentally can be used for determination of the parameters τ/\mathcal{A} and μ .

The above theoretical results are compared in Fig. 4 with the experimental data obtained on a large ($d \cong 1$ mm) $\text{YBa}_2\text{Cu}_3\text{O}_7$ crystal. The relaxation of the magnetic moment was fitted by the direct numerical solution of Eqs. (14) and (21), where τ/\mathcal{A} , j_c , μ and U_c were considered as independent fitting parameters. Thus $U(t)$ -dependence is found directly from the experiment and is compared in Fig. 4 with the theoretical curve found from Eq. (22) with the same parameters. The experimental and theoretical results almost coincide, and the characteristic maximum in $d(U/kT)/d\ln t$ at $t \cong 10\tau/\mathcal{A}\mu$ is very clear.

C. Creep at $j_c = \text{const}$, $U = U_0(B/B_0)(j_c/j - 1)$

Consider this simplest model dependence of U on B and j , which can mostly be analyzed analytically before a more complicated case of collective creep. We have changed the notation U_0 instead of U_c , as in the previous subsections, for reasons which are clarified below. Fig. 5

illustrates the numerical solution for $B(x)$ and $U(x)$ profiles in the case. One observes that the general condition $U \cong \text{const}$ holds in this case as well as in the previous one, where U was independent of B . The same narrow peak in U is located at the center of the sample $x = 0$, as described in Section II. Since U depends only on the ratio U_0/B_0 , we can choose B_0 arbitrarily. It is most convenient to accept $B_0 \equiv H^*$. Then, using the Maxwell equation (9) and the condition $U \cong \text{const}$, one obtains the approximate expression for the field profile in the sample:

$$\frac{x}{d} \cong 1 + \frac{B - H}{H^*} + \frac{U}{U_0} \ln \frac{B}{H}. \quad (25)$$

Denoting the field at the center of the sample as $B(0)$, which is found from Eq. (25) at $x = 0$, one can rewrite the magnetic moment m (see Eq. (12)), as:

$$m = \frac{1}{d} \int_{B(0)}^H x dB. \quad (26)$$

Then

$$\frac{\partial m}{\partial t} = \frac{\partial m}{\partial U} \frac{\partial U}{\partial t} = -\frac{1}{U_0} \left[\ln \frac{H}{B(0)} - H + B(0) \right] \frac{\partial U}{\partial t}.$$

On the other hand, as follows from Eq. (13),

$$\frac{\partial m}{\partial t} = -\frac{\mathcal{A}}{4\tau} \left| \frac{\partial B}{\partial x} \right|_{x=\pm d} \exp(-U/kT), \quad (27)$$

and one gets an equation which determines the activation energy:

$$\frac{dU}{dt} = \frac{\mathcal{A}U_0}{\tau} \frac{h}{2(h+u)[h-b(0)-b(0)\ln(h/b(0))]} \exp(-U/kT), \quad (28)$$

where we denoted $h = H/H^*$, $b = B/H^*$, and $u = U/U_0$. This cumbersome expression can be reduced if one uses the expansion over $\Delta = [H - B(0)]/H$, which becomes exact at $\Delta \rightarrow 0$, but actually holds with 10% accuracy at worst for all $\Delta < 1$, i.e., for all $B(0) < H$.

Then one gets:

$$\frac{dU}{dt} \cong \frac{\mathcal{A}}{\tau} (U + U_c) \left(1 + \frac{2}{3}\Delta \right) \exp(-U/kT), \quad (29)$$

where $U_c = hU_0$. This result differs from Eq. (23) only by the correction factor $1 + 2\Delta/3$. This means that the results of the previous subsection, where U was field independent, apply here just by accounting for the correction factor $1 + 2\Delta/3$, which in most cases is not of great importance.

Eq. (29) enables us to find the $U(t)$ -dependence, and then, using Eq. (25) we get the field profile $B(x)$ as a function of time, i.e., solve the creep problem completely. We call such an approach as "semi-analytical" solution. Its results are compared in Fig. 5a with the exact solution obtained by a direct numerical integration of Eq. (10) with no assumptions on constancy of U . One observed that the semi-analytical solution, being much less time-consuming (note that the solution of Eq. (29) is quite universal and has been already obtained in the previous subsection), provides a perfect fit to the exact description of the creep process.

D. Creep at $j_c = \text{const}$, $U = U_0(B/B_0)^\alpha (j_c/j)^\mu$ (collective creep)

This is the general dependence of U on B and j in the collective creep theory [2] for $j \ll j_c$. The spatial constancy of U holds in this case as well as in previously considered cases. We have checked it numerically for various α and μ . The condition $U \cong \text{const}$ together with the Maxwell equation (9) determines the field profile:

$$h^\nu - b^\nu \cong \frac{\nu}{u^{1/\mu}} \left(1 - \frac{x}{d}\right), \quad (30)$$

where we denote $\nu = 1 - \alpha/\mu$ and assume $B_0 = H^*$, as in the previous case. Here we take $\alpha \neq \mu$ (the case $\alpha = \mu$ is almost identical to that considered in the previous subsection). The field $b(0)$ is determined, as follows from Eq. (30), by $h^\nu - b(0)^\nu = \nu/u^{1/\mu}$. The magnetic moment can be calculated using Eq. (26):

$$m = H^* \left[h - \frac{u^{1/\mu}}{\nu + 1} (h^{\nu+1} - b(0)^{\nu+1}) \right], \quad (31)$$

and, using Eq. (27), one gets:

$$\frac{dU}{dt} = \frac{\mathcal{A}\mu(\nu + 1)}{2\tau h^{\nu-1} u^{2/\mu}} [h^{\nu+1} - b(0) (h^\nu + u^{-1/\mu})]^{-1} U \exp(-U/kT). \quad (32)$$

This expression, being a bit cumbersome, can be reduced using the expansion over $\Delta = (H - B(0))/H$, which, as in the previous case, works with reasonable accuracy (better than 10%) at all $B(0) \lesssim H$:

$$\frac{dU}{dt} = \frac{\mathcal{A}\mu}{\tau} U \left[1 + \frac{2\alpha}{3\mu} \Delta \right] \exp(-U/kT). \quad (33)$$

This result is very similar to Eq. (29). The absence of U_c in Eq. (33) corresponds to the absence of term -1 in the dependence of the activation energy U on j in this model (compared with the two previous cases). The factor in the square brackets in Eq. (33) describes the effective renormalization of U in the pre-exponential factor resulting from the dependence of U on B . If $\alpha = 0$, which means that U is independent of B , then the renormalization disappears. The same happens at $B(0) \rightarrow H$. At $\alpha = \mu$ the correction factor reduces to $1 + 2\Delta/3$, which is consistent with the previous case, where $\alpha = \mu = 1$.

In Fig. 6 we compare the direct numerical solution of Eq. (10) with the semi-analytical one determined by Eqs. (30)-(31). Fig. 6a shows the numerical (exact) $B(x)$ profiles compared with Eq. (30), and Fig. 6b shows $m(\ln t)$, obtained numerically from Eq. (10) and semi-analytically from Eqs. (30)-(33). The quality of the semi-analytical approach is perfect in this case as well as in the previous one.

In the most general case:

$$U = U_0(B/B_0)^\alpha [(j_c/j)^\mu - 1] \quad (34)$$

one gets an expression which naturally conforms to Eqs. (29) and (33):

$$\frac{dU}{dt} = \frac{\mathcal{A}\mu}{\tau} (U + U_c) \left[1 + \frac{2\alpha}{3\mu} \Delta \right] \exp(-U/kT), \quad (35)$$

where, as above, $U_c = hU_0$. We skip the cumbersome derivation of the last expression, which requires expansion over Δ starting from the equation for the field profile $B(x)$. The generalized logarithmic solution of this equation acquires the form

$$U = kT \ln \left(1 + \frac{\mathcal{A}\phi_0 H \mu (U + U_c) [1 + (2\alpha/3\mu)\Delta]}{2\pi\eta d^2 kT} t \right), \quad (36)$$

which coincides with Eq. (1) if

$$t_0 = \frac{2\pi\eta d^2 kT}{\mathcal{A}\phi_0 H\mu(U + U_c)[1 + (2\alpha/3\mu)\Delta]} = \frac{H^*}{H} t_H, \quad (37)$$

where we introduced $t_H \equiv t_0(H = H^*)$. Note that t_H is almost field independent, since H enters t_H only via Δ . Note that both t_0 and t_H depend on time via U and the correction term (in square brackets).

E. Creep at $j_c = j_c(B) \neq const$

Above, we have considered only $j_c = const$. However, the field dependence of the critical current, $j_c = j_c(B)$, does not violate the general condition, Eq. (2), of self-organization of flux creep. As a direct consequence of this condition it is worth mentioning the following: If the dependence of U on j and B has the form: $U \propto f(j_c(B)/j)$, where f is an arbitrary function, then the spatial constancy of U results in establishing of a "partial" critical state [21] with $j \propto j_c(B)$. For instance, if the critical current obeys the Kim dependence $j_c(B) = j_0 B_0 / (B_0 + B)$, then the field profile $B(x)$ during the relaxation should be determined by the condition $j = p j_0 B_0 / (B_0 + B)$ with $0 < p < 1$.

However, for more complicated dependencies of U on B and j this is not the case, and the profiles $B(x)$ can differ significantly from that in the critical state. In the next Section we consider an example of such a behavior.

IV. SEMI-ANALYTICAL SOLUTIONS FOR ANOMALOUS MAGNETIZATION (FISHTAIL).

The equation (35) and its reduced forms (see Eqs. (29) and (33)), which are just ordinary differential equations, present the method of semi-analytical integration of the equation for flux motion (see Eq. (10)), for the case of collective creep, where the dependence of U on B and j is described by Eq. (34), or by its reduced versions. Of course an analogous solution can be found for any $U(B, j)$ -dependence, not only for that described by Eq. (34). This

semi-analytical approach provides a good fit to the exact solution, obtained by numerical integration of Eq. (10), as one can see in Fig. 6. The correction factor $1 + (2\alpha/3\mu)\Delta$ can be neglected except for short times $t \gtrsim \tau/\mathcal{A}\mu$.

The semi-analytical solutions can be applied for the description of an anomalous magnetization, coined a "fishtail", found in clean high- T_c superconductors [6–8]. Note that j_c enters Eq. (35) only via the correction factor which is negligible in most cases, especially at high fields $H \gg H^*$ where $\Delta \ll 1$. Thus the solution $U(t)$ of Eq. (35) is determined by the current exponent μ (and not by the field one, α), by the characteristic energy U_c , and by τ (which in turn depends on d , η and H). If one measures the magnetization current j at the edge of the sample, where $U(B, j) = U(H, j)$ as a function of H , keeping the time window t of the experiment constant for each H (this is the case for most studies of fishtails), then U along the measured line $M(H)$ or $j(H)$ can be written, as follows from Eq. (36), as

$$U(H, t)/kT - \ln(U + U_c) \cong \ln H + \ln t + \ln \left(\frac{\mathcal{A}\phi_0\mu [1 + (2\alpha/3\mu)\Delta]}{2\pi\eta d^2 kT} \right), \quad (38)$$

where the last term in Eq. (38) almost does not depend on H and t . This means that the magnetization curve is determined by:

$$\frac{dU}{kT} - \frac{dU}{U + U_c} = \frac{dH}{H}. \quad (39)$$

In Fig. 7 we present the results of our semi-analytical approach to the problem of dynamic fishtail formation taking $j_c(B) = j_0 B_c / (B_c + B)$ (Kim model) and collective creep with

$$U = U_0 (B/H^*)^\alpha \left[\left(\frac{j_c(B)}{j} \right)^\mu - 1 \right] \left(\frac{B_c + B}{B} \right)^\mu. \quad (40)$$

The last factor in this equation is added to cancel the dependence of j_c on B and keep the general collective creep condition: $U \propto B^\alpha j^{-\mu}$ for $j \ll j_c$. At each H we find the energy U down to where the system relaxes during the "experimental" time window t , and then, using this U , we determine the corresponding $j_{x=\pm d}$ according to Eq. (40). The results show a clear fishtail due to fast relaxation at low fields (see Fig. 7).

Note that Eq. (40) provides an example of the case where the field profiles $B(x)$ are significantly different from the critical one at $j = j_c$, and a "partial critical state" [21] is not established.

Since $dU = (\partial U/\partial H)dH + (\partial U/\partial j)dj$, one obtains using Eq. (39) that the magnetization curve (fishtail) is determined by the condition:

$$\frac{dj}{dH} = - \left(\frac{\partial U}{\partial H} - \frac{kT}{H} \frac{U + U_c}{U + U_c - kT} \right) \left(\frac{\partial U}{\partial j} \right)^{-1}. \quad (41)$$

For the case of collective creep, where $U \propto H^\alpha j^{-\mu}$, we have $\partial U/\partial H = (\alpha/H)U$ and $\partial U/\partial j = -(\mu/j)U$. Then, taking into account that $U + U_c \gg kT$, we get

$$\frac{dj}{dH} \cong \frac{\alpha}{\mu} \frac{j}{H} \left(1 - \frac{1}{\alpha} \frac{kT}{U} \right). \quad (42)$$

The peak of the fishtail, where $j(H)$ reaches maximum, corresponds to $U \cong kT/\alpha$, as follows from Eq. (42). This implies that j increases as a function of H until it almost reaches the $j_c(H)$ curve. Far below j_c , where $kT/\alpha U \ll 1$, one gets from Eq. (42) that $j \propto H^{\alpha/\mu}$.

We see from Eqs. (38) and (39) that U changes along the magnetization curve obtained at a fixed time window t . However, one can measure $j_{Ht}(H)$ keeping the product Ht as constant, which, according to Eq. (36), should result in a constant U along the magnetization curve (neglecting the correction factor $1 + (2\alpha/3\mu)\Delta$). The difference $j_{Ht}(H) - j(H)$, where $j(H)$ is taken at $t = \text{const}$, is determined by:

$$\frac{d(j_{Ht} - j)}{dH} \cong - \frac{kT}{H (\partial U/\partial j)}, \quad (43)$$

which provides a tool for independent analysis of $U(j)$ -curve.

Above in this Section we have considered the exponents α and μ to be constants. However, different regions in the $j - H$ diagram correspond to different relaxation regimes, such as single vortex creep, small and large bundle creep, etc. (see [2–4]). The energy scale U_0 , as well as the exponents α and μ may vary significantly from one region of $j - H$ to another. As one observes from Eq. (36), the crucial exponent of the above two is μ . Its rapid change at the boundary between the creep regions from μ_1 to μ_2 is equivalent to a change of H by

factor μ_2/μ_1 . As follows from Eq. (38), this results in a change of $\simeq \ln(\mu_2/\mu_1)$ in U/kT at the boundary between two creep regions. Thus U does not change much at the crossover from one pinning regime to another. However, j (and, in turn, M) can be changed significantly at such a boundary, since for different relaxation laws (different U_c , α and μ) the same U is reached at significantly different j . As H increases, the growing vortex bundles lead to increase of characteristic energies U_c , thus one should expect a step-like increase of j when crossing the boundaries *single vortex pinning* \rightarrow *small bundles* \rightarrow *large bundles*.

If one measures the exponent μ along the magnetization curve (see, for instance, Ref. [7]), then a curve of constant U in the $H - j$ diagram can be plotted using rather $t \propto (\mu H)^{-1}$ instead of $t \propto H^{-1}$, as was suggested above.

V. RELAXATION IN THE REMANENT STATE AND ANNIHILATION LINES

A particular and very interesting case, where the discussed above self-organization of the flux motion should be modified significantly, is relaxation in the presence of annihilation lines $B = 0$. The vortices and antivortices approach the annihilation line from different sides and annihilate each other. The arguments of Section II for the constancy of U are not valid in this case, at least in the vicinity of the annihilation lines (see comment at the end of Section II). Therefore, this case should be studied separately.

Consider the simplest situation of remanent relaxation, where the field has been ramped up and then instantaneously removed, so $B = 0$ at the edges $x = \pm d$ of the slab. There are no antivortices in this case, since the annihilation line coincides with the edge of the sample.

The description of the flux motion in this case using Eq. (3) looks self-contradictory since at the sample edge $B = 0$, whereas the magnetic flux current $D = Bv$ is finite at the edges and, moreover, obviously should reach there its maximal value over the sample. However, the contradiction is void provided the field vanishes at the sample edge as $B \propto \sqrt{d - x}$, i.e., proportional to the square root of the distance to the edge (see Fig. 8). At the same time the vortex velocity diverges at the sample edge as $v \propto \partial B/\partial x \propto 1/\sqrt{d - x}$. This divergency

is removed by an appropriate cut-off for $d - x$, which we discuss later in this Section, but inevitably leads to the appearance of the flux-flow region near the edge or, most generally, near the annihilation line. However $D \propto B(\partial B/\partial x)$ remains finite and continuous with no singularity at the edge. This is confirmed by direct computer simulations of the relaxation in the remanent state (see Fig. 8).

Let us estimate the coefficient k in the square-root dependence $B_{edge} \cong k\sqrt{d-x}$ near the sample edge, which should include the flux flow region $U = 0$. The magnetic flux current reaches at $x = d$ its maximum over the sample: $D_{x=d} = (\phi_0/4\pi\eta) [B \partial B/\partial x]_{x \rightarrow d} = \phi_0 k^2/8\pi\eta$, but remains of the same order as the mean flux current $\langle D \rangle$ over the sample: $D_{x=d} = \mathcal{C} \langle D \rangle$, where $\mathcal{C} \gtrsim 1$ is a numerical factor. Estimating $\langle D \rangle \simeq (\mathcal{A}\phi_0/4\pi\eta) \langle B \rangle \langle \partial B/\partial x \rangle \exp(-\langle U \rangle/kT)$, $\langle B \rangle \simeq B(0)/2$, $\langle \partial B/\partial x \rangle \simeq B(0)/d$, one gets $k \simeq B(0)\sqrt{\mathcal{C}\mathcal{A}\exp(-\langle U \rangle/kT)/d}$. Note that the above estimation is based on the constancy of U , i.e., $U \cong \langle U \rangle$ throughout the sample except the edge flux-flow regions, which we assume to be small. Thus we get:

$$B_{edge}(x) \cong B(0)\sqrt{\mathcal{C}\mathcal{A}\exp(-\langle U \rangle/kT)\frac{d-x}{d}}. \quad (44)$$

A natural cut-off for the area of applicability of Eq. (44) is: $d - x > \lambda$, otherwise the surface effects such as Bean-Livingston interaction with the surface [26] should be accounted for. There are additional restrictions: (i) the current cannot exceed the depairing one: $j = (c/4\pi)\partial B/\partial x < j_d$; and (ii) the intervortex distance $a \simeq \sqrt{\phi_0/B(x)}$ should not exceed the distance to the surface $d - x$ at any x . It can be easily confirmed that the condition $d - x > \lambda$ is stronger than the other two at most reasonable values of $B(0)$ and d .

Let us call the region $\tilde{x} < |x| < d$ near the sample edges, where the activation energy grows from $U = 0$ at the very edge (flux-flow region) up to $U(\tilde{x}) \cong \langle U \rangle$, as the area of "annihilation dominated" organization of flux creep. Its width $d - \tilde{x}$ can be estimated as follows: We substitute Eq. (44) into the collective creep formula for $U(B, j)$, see Eq. (34), and find \tilde{x} where U reaches its mean value $\langle U \rangle$. This is of course a crude approximation, since Eq. (44) is valid in the flux-flow region only, and for the whole "annihilation dominated" region it

provides an underestimation for B and, in turn, j . After straightforward calculations we get:

$$\frac{d - \tilde{x}}{d} \simeq \left(\frac{\langle U \rangle}{U_0} \right)^{\frac{2}{\alpha + \mu}} \exp \left(\frac{\alpha - \mu \langle U \rangle}{\alpha + \mu kT} \right). \quad (45)$$

The above result implies that the width $d - \tilde{x}$ of the "annihilation dominated" region is crucially dependent upon the relationship between the exponents α and μ . For $\mu > \alpha$ and $\langle U \rangle \gg kT$ this region appears to be exponentially small, i.e., $\tilde{x} \cong d$. Computer simulations show a step-like increase of U at the edge to the value comparable with $\langle U \rangle$, and then U grows smoothly and slowly towards the center of the sample (see Fig. 9a). Though δU appears to be significantly greater than for the case of finite H , discussed in previous Sections, even here U does not vary significantly: $\delta U \lesssim 4kT$ in the whole sample, excluding the sharp step at the edge. For the opposite case, $\mu < \alpha$, one finds from Eq. (45) the unphysical result that $(d - \tilde{x})/d$ is exponentially large though, of course, $(d - \tilde{x})/d < 1$ anyway. This implies that our assumption about the spatial constancy of $U(x) \cong \langle U \rangle$ throughout almost the whole sample (except small edge regions) is self-contradictory in this case. Thus for $\mu < \alpha$ the effect of the annihilation line spreads over the whole sample, and there is not any evidence of constancy of U . This is confirmed by numerical simulations (see Fig. 9b). The boundary case, where $\mu = \alpha$, is illustrated in Fig. 9c.

VI. CONCLUSION

We considered the generalization of the logarithmic solution Eq. (1) for flux creep at different dependencies of the activation energy U on field B and current j and confirmed it by numerical analysis. The general condition which governs the relaxation is $U(x) \cong \text{const}$ throughout the sample, and this result holds at any particular $U(B, j)$ -dependence. This results from a *self-organization* of flux creep in the undercritical state $j < j_c$, which implies that the influence of all the creep parameters, B , j and U , on the relaxation rate should be of the same order of magnitude. This self-organization should not be mixed with the *self-organized criticality* of flux motion at $j \cong j_c$.

For U independent of B , i.e., $U = U(j)$, we restore the known result of straightness ($j \simeq \text{const}$) of the field profiles throughout the sample. For the case where U essentially depends on B the condition of spatial constancy of $U(B, j)$ determines the one-parameter family of field profiles $B_U(x)$ and enables us to find a semi-analytical solution for $U(t)$ and, in turn, for time evolution of the field profiles $B_U(x)$, i.e., to solve the creep problem completely. Such a semi-analytical solution provides a perfect fit to the exact numerical solution (obtained without any assumptions on constancy of U) and appears to be quite useful for the description of the dynamic development of anomalous magnetization (fishtail) due to fast relaxation rates at low fields.

The effect of the annihilation lines $B = 0$ on the self-organization of the collective creep where $U \propto B^\alpha j^{-\mu}$ (see Eq. (34)) is crucially dependent on the relationship between α and μ . At $\alpha < \mu$ the effect is just an increase of variation δU over the sample, with a step-like vanishing of U in the very narrow regions of flux flow in the vicinity of an annihilation line. However, for $U \gg kT$ we still get $\delta U \ll U$, i.e., the condition $U \cong \text{const}$ holds qualitatively in this case. At $\alpha > \mu$ the above condition no longer holds, and the presence of an annihilation line destroys the self-organization in the whole sample irrespective of its size.

Acknowledgments.

The authors are grateful to V. M. Vinokur for critical reading of the manuscript and valuable discussions. L. B. acknowledges support from the Israel Academy of Sciences and from the German-Israeli Foundation (GIF).

REFERENCES

- [1] Y. Yeshurun and A. P. Malozemoff, Phys. Rev. Lett. **60**, 2202 (1988).
- [2] G. Blatter, M. V. Feigel'man, V. B. Geshkenbein, A. I. Larkin, and V. M. Vinokur, Rev. Mod. Phys. **66**, 1125 (1994).
- [3] Y. Yeshurun, A. Shaulov, and A. P. Malozemoff, Rev. Mod. Phys. **68**, 911 (1996).
- [4] E. H. Brandt, Rep. Prog. Phys. **58**, 1465 (1995).
- [5] V. B. Geshkenbein and A. I. Larkin, Sov. Phys. JETP **68**, 639 (1989).
- [6] M. Daeumling, J. M. Seutjens, and D. C. Larbalestier, Nature (London) **346**, 332 (1990); L. Krusin-Elbaum, L. Civale, V. M. Vinokur, and F. Holtzberg, Phys. Rev. Lett. **69**, 2280 (1992); S. N. Gordeev, W. Jahn, A. A. Zhukov, H. K pfer, and T. Wolf, Phys. Rev. B **49**, 15420 (1994); Y. Yeshurun *et al.*, Proc. of the 7th International Workshop on "Critical Currents in Superconductors", Alpbach, Austria, 1994, p. 237; L. Klein, E. R. Yacoby, Y. Yeshurun, A. Erb, G. Muller-Vogt, V. Breit, and H. W hl, Phys. Rev. B **49**, 4403 (1994); H. K pfer, S. N. Gordeev, W. Jahn, R. Kresse, R. Meier-Hirmer, T. Wolf, A. A. Zhukov, K. Salama and D. Lee, Phys. Rev. B **50**, 7016 (1994); A. A. Zhukov, H. K pfer, G. Perkins, L. F. Cohen, A. D. Caplin, S. A. Klestov, H. Claus, V. I. Voronkova, T. Wolf, and H. W hl, Phys. Rev. B **51**, 12704 (1995).
- [7] Y. Abulafia, A. Shaulov, Y. Wolfus, R. Prozorov, L. Burlachkov, Y. Yeshurun, D. Majer, E. Zeldov, H. W hl, V. B. Geshkenbein and V. M. Vinokur, Phys. Rev. Lett. **77**, 1956 (1996).
- [8] D. Giller, A. Shaulov, R. Prozorov, Y. Abulafia, Y. Wolfus, L. Burlachkov, Y. Yeshurun, E. Zeldov, V. M. Vinokur, J. L. Peng, and R. L. Greene, Phys. Rev. Lett. **79**, 2542 (1997).
- [9] Y. Yeshurun, N. Bontemps, L. Burlachkov, and A. Kapitulnik, Phys. Rev. B **49**, 1548 (1994).

- [10] M. V. Feigel'man, V. B. Geshkenbein, and V. M. Vinokur, Phys. Rev. B **43**, 6263 (1991).
- [11] C. P. Bean, Phys. Rev. Lett. **8**, 250 (1962); Rev. Mod. Phys. **36**, 31 (1964).
- [12] C. J. van der Beek, G. J. Nieuwenhuys, and P. H. Kes, Physica C **185-189**, 2241 (1991).
- [13] P. Bak, C. Tang, and K. Wisenfeld, Phys. Rev. Lett. **59**, 381 (1987); Phys. Rev. A **38**, 364 (1988); C. Tang and P. Bak, Phys. Rev. Lett. **60**, 2347 (1988).
- [14] O. Pla and F. Nori, Phys. Rev. Lett. **67**, 919 (1991); C. Tang, Physica A **194**, 315 (1993); Z. Wang and D. Shi, Phys. Rev. B **48**, 4208 (1993); W. Pan and S. Doniach, Phys. Rev. B **49**, 1192 (1994); S. Field, J. Witt, F. Nori, and X. Ling, Phys. Rev. Lett. **74**, 1206 (1995).
- [15] M. R. Beasley, R. Labusch, and W. W. Webb, Phys. Rev. **181**, 682 (1969).
- [16] J. Bardeen and M. J. Stephen, Phys. Rev. **140**, 1197A (1965); see also M. Tinkham, *Introduction to Superconductivity*, McGraw-Hill, New-York, 1975.
- [17] Y. Abulafia, A. Shaulov, Y. Wolfus, R. Prozorov, L. Burlachkov, Y. Yeshurun, D. Majer, E. Zeldov, and V. M. Vinokur, Phys. Rev. Lett. **75**, 2404 (1995).
- [18] E. Zeldov, J.R. Clem, M. McElfresh, and M. Darwin, Phys. Rev. B **49**, 9802 (1994).
- [19] M. Buttiker and R. Landauer, Phys. Rev. A **23**, 1397 (1981).
- [20] V. M. Vinokur, M. V. Feigel'man, and V. B. Geshkenbein, Phys. Rev. Lett. **67**, 915 (1991).
- [21] C. J. van der Beek, G. J. Nieuwenhuys, P. H. Kes, H. G. Schnack and R. Griessen, Physica C **197**, 320 (1992).
- [22] V. V. Bryksin and S. N. Dorogovtsev, JETP **77**, 791 (1993).
- [23] John Gilchrist and C. J. van der Beek, Physica C **231**, 147 (1994).
- [24] H. G. Schnack, R. Griessen, J. G. Lensink, C. J. van der Beek, and P. H. Kes, Physica

C **197**, 337 (1992).

[25] M. Golosovsky, M. Tsindlekht, H. Chayet, and D. Davidov, Phys. Rev. B **50**, 470 (1994).

[26] C. P. Bean and J. D. Livingston, Phys. Rev. Lett. **12**, 14 (1964).

FIGURE CAPTIONS

Fig. 1 a) The field profiles $B(x)$ for flux flow (dashed lines) and creep (squares) for $U = U_0 [(j_c/j) - 1]$ with $H^* = H/2$. The critical state ($j = j_c$) and the full penetration state ($j = j^*$) are shown in solid black and grey lines, respectively. Note an almost exact formation of a critical state at the crossover flow \rightarrow creep.

b) Spatial dependence of U at different times t/τ_{flow} . Note almost spatial constancy of U except narrow regions $x \cong 0$.

Fig. 2 Relaxation of j can be imagined as a motion of a dot along the $U(j)$ -curve (solid). For the logarithmic approximation $U(j)$ is substituted by its tangent line (dashed). Time t_0 corresponds to the "motion" along the negative part ($U < 0$) of the line, whereas τ_{flow} corresponds to the "motion" from $j = \infty$ down to $j = j_c$ along $U = 0$.

Fig. 3 Comparison of "pure" logarithmic (triangles), straightforward (circles) and generalized logarithmic (solid line) solutions of Eq. (19), which were derived under assumption $U(x) = const$, together with the "exact" numerical solution (squares) of Eq. (10) for $U(j) = U_c [(j_c/j)^\mu - 1]$. Open and filled symbols correspond to U/kT and $d(U/kT)/d \ln t$, respectively. Note that all the solutions except the pure logarithmic one show a maximum in $dU/d \ln t$ at $\mathcal{A}\mu t/\tau \gtrsim 1$.

Fig. 4 Experimentally obtained relaxation rate $d(U/kT)/d \ln t$ (triangles) and normalized magnetic moment M/M_c , which is equal to j/j_c (circles) vs. t and their fit by the

generalized logarithmic solution at the same values of parameters: $\mathcal{A}/\tau = 0.03 \text{ sec}^{-1}$, $U_c/kT = 12.62$ and $\mu = 2.03$.

Fig. 5 a) The field profiles $B(x)$ for flux creep at $U = U_0(B/H^*)(j_c/j - 1)$ with $H^* = H/2$ found by numerical solution of Eq. (10) (squares) and by the semi-analytical approach (solid lines).

b) $U(x)$ found for the same $U(B, j)$ -dependence from the numerical solution of Eq. (10).

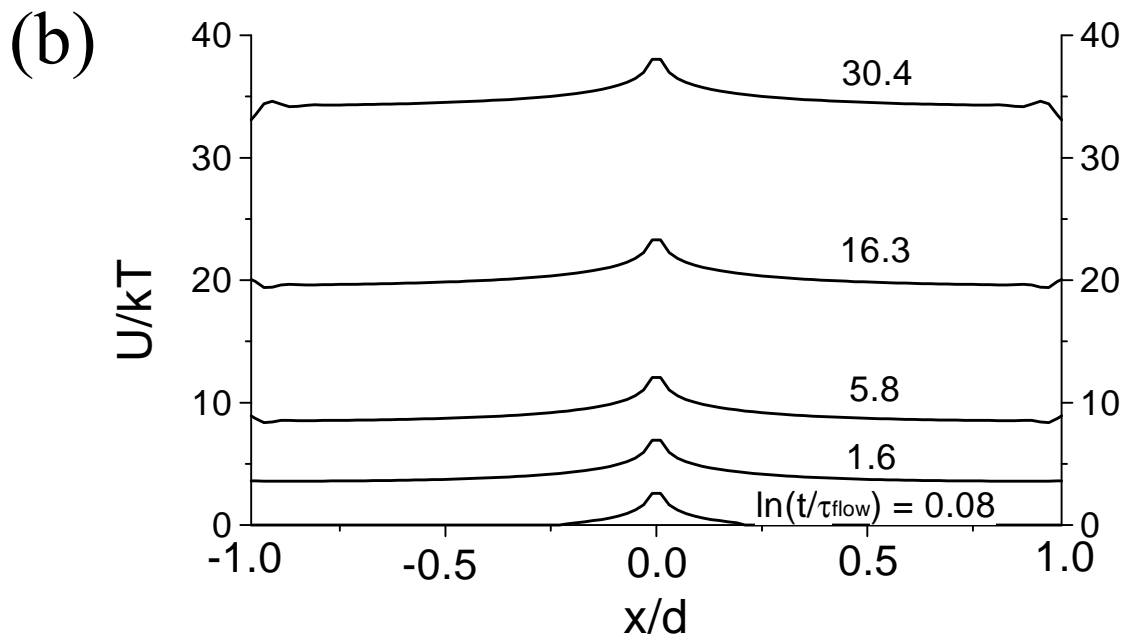
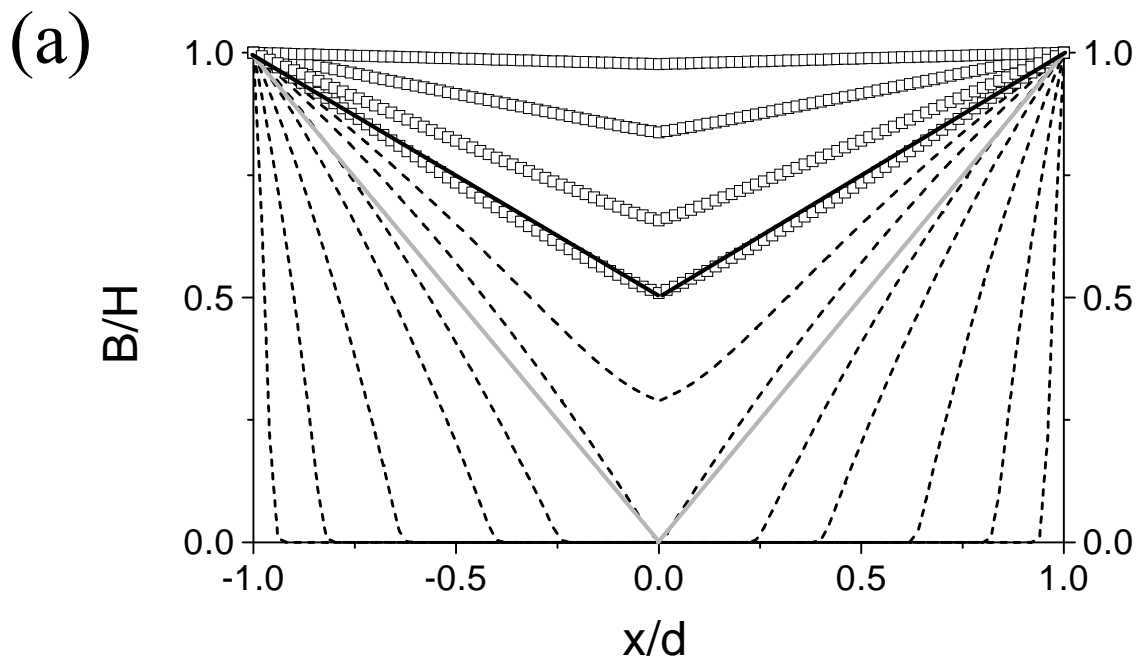
Fig. 6 a) The same as in Fig. 5a for the collective creep dependence $U = U_0(B/H^*)^\alpha(j_c/j)^\mu$ with $\alpha = 1$, $\mu = 2$ and $H^* = H/2$.

b) Magnetization for the same $U(B, j)$ -dependence found from the numerical solution of Eq. (10) (circles) and by semi-analytical approach (solid line). For $m/H < 0.1$ the circles and the line completely coincide.

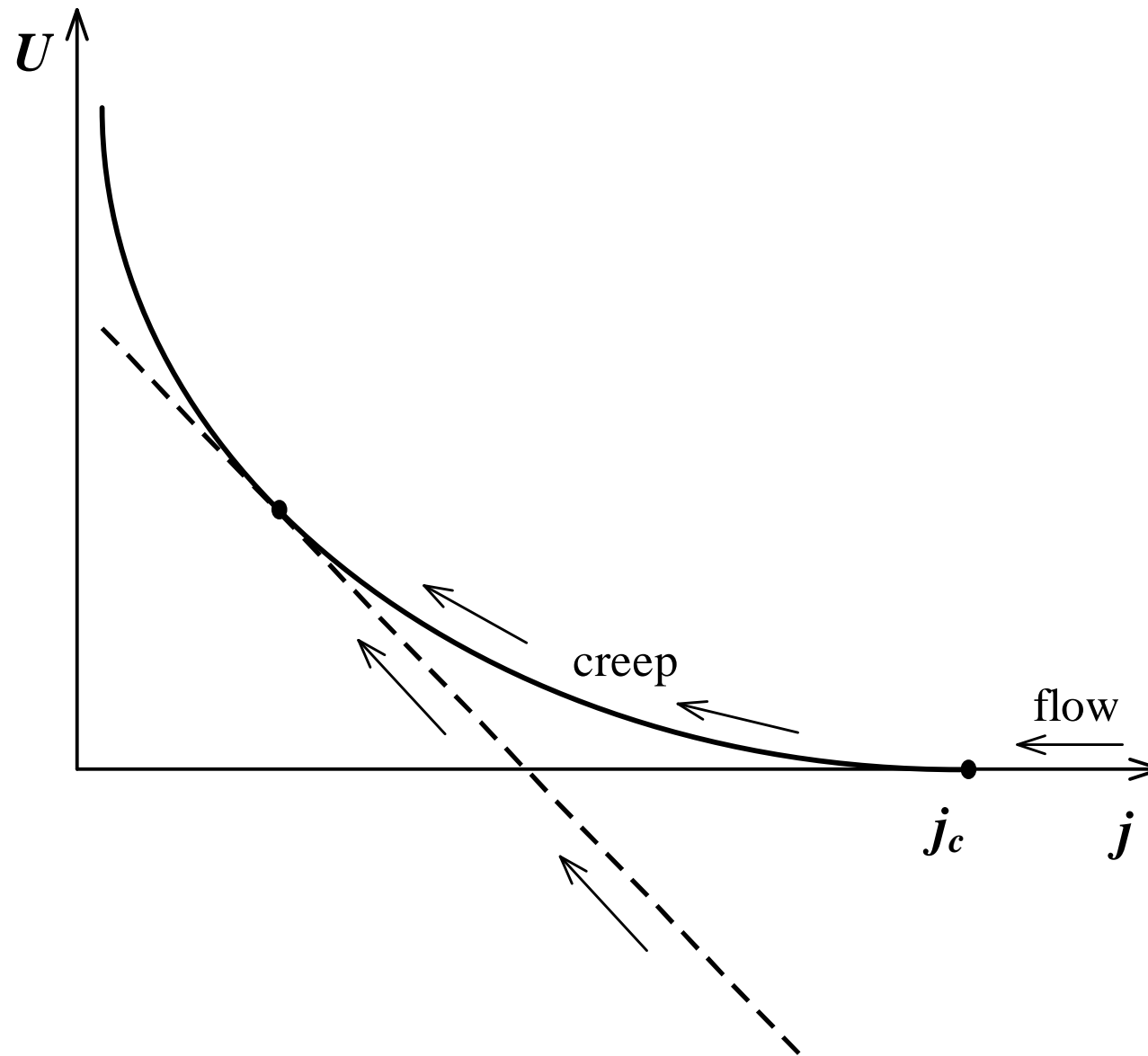
Fig. 7 Dynamic development of anomalous magnetization (fishtail) found by the semi-analytical solution of the Kim model (see Eq. (40)) with $B_c = 2H^*$, $\alpha = 1$ and $\mu = 2$. Relaxation starts at $t = 0$ from $j_c(H) = j_0 B_c / (B_c + H)$ shown as dashed line. Due to faster relaxation at small H an anomalous magnetization develops at $j \ll j_c$. Circles and solid lines correspond to the direct numerical and semi-analytical solutions, respectively, for $\ln(t/\tau_{flow}) = 2.8, 7.4$ and 14.3 .

Fig. 8 The magnetic induction B (squares), vortex velocity v (circles) and the magnetic current $D = Bv$ (triangles) vs. $d - x$ found numerically from Eq. (11) near the sample edge $x = d$. The fits are: $\sqrt{d - x}$ for B and $1/\sqrt{d - x}$ for v . Note that D shows no peculiarity at $x = d$.

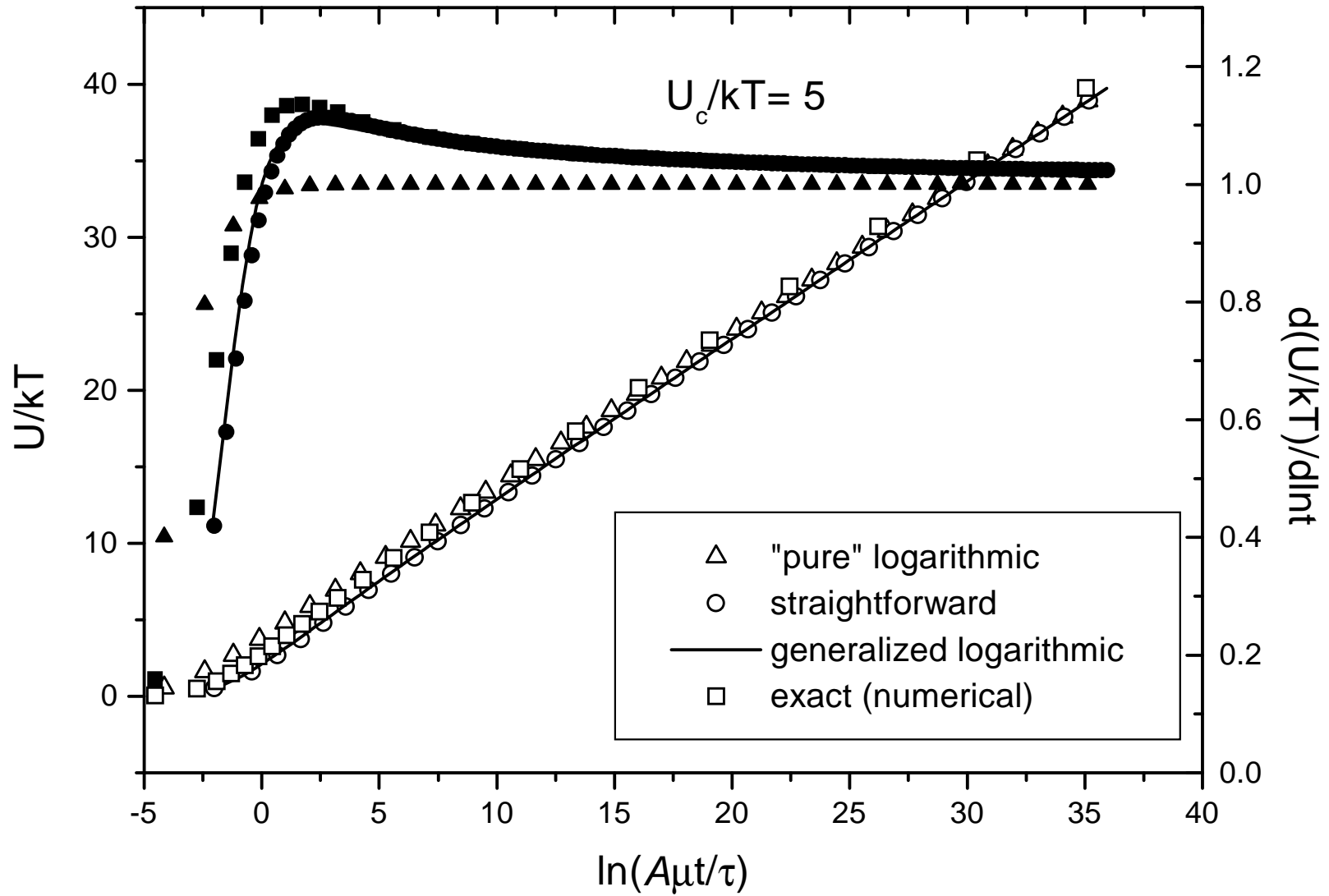
Fig. 9 The activation energy U/kT in the remanent state: a) $\alpha = 0.1$, $\mu = 1$; b) $\alpha = 1.5$, $\mu = 0.5$ c) $\alpha = 1$, $\mu = 1$.



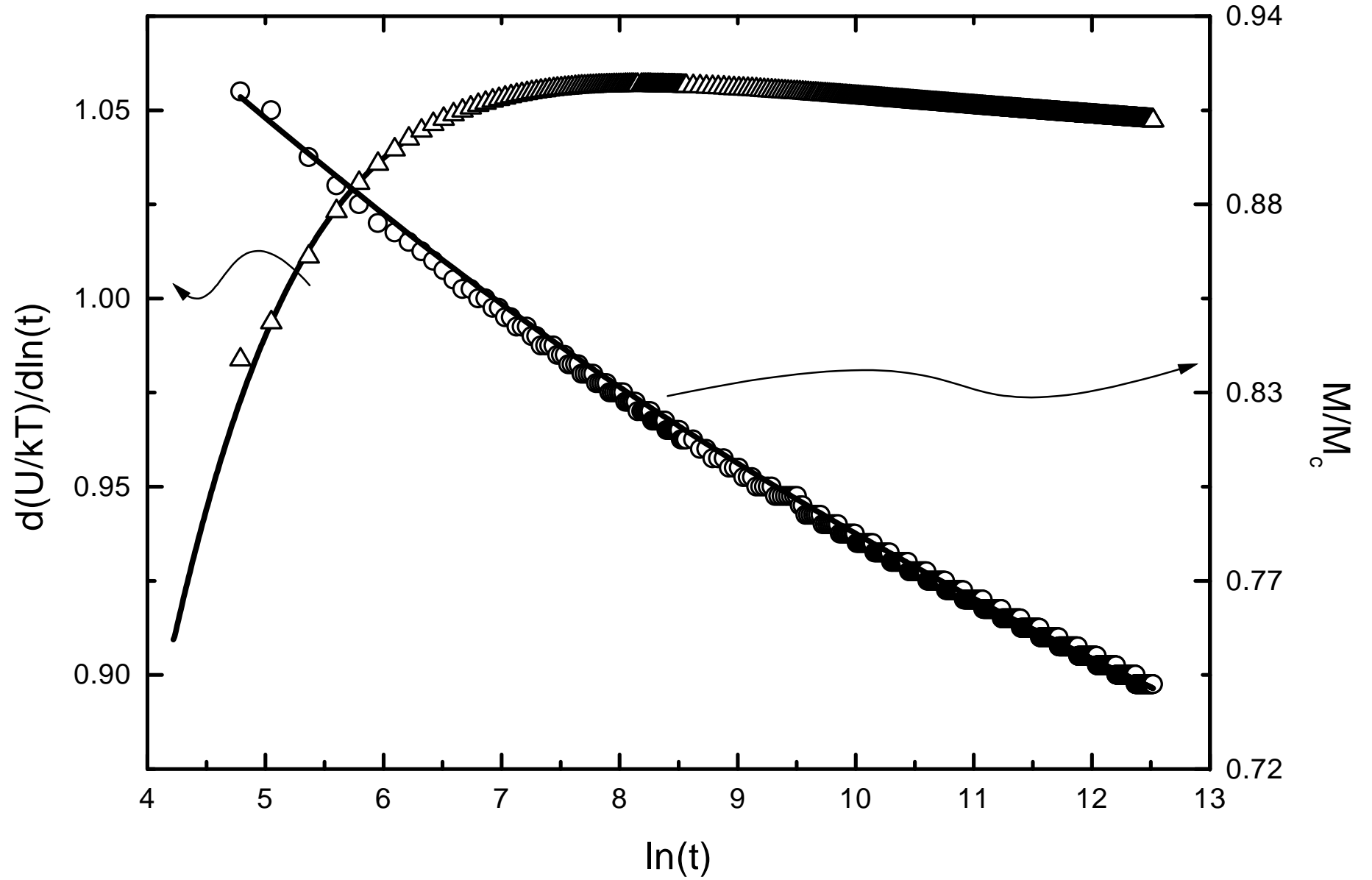
Burlachkov *et al.* Fig. 1



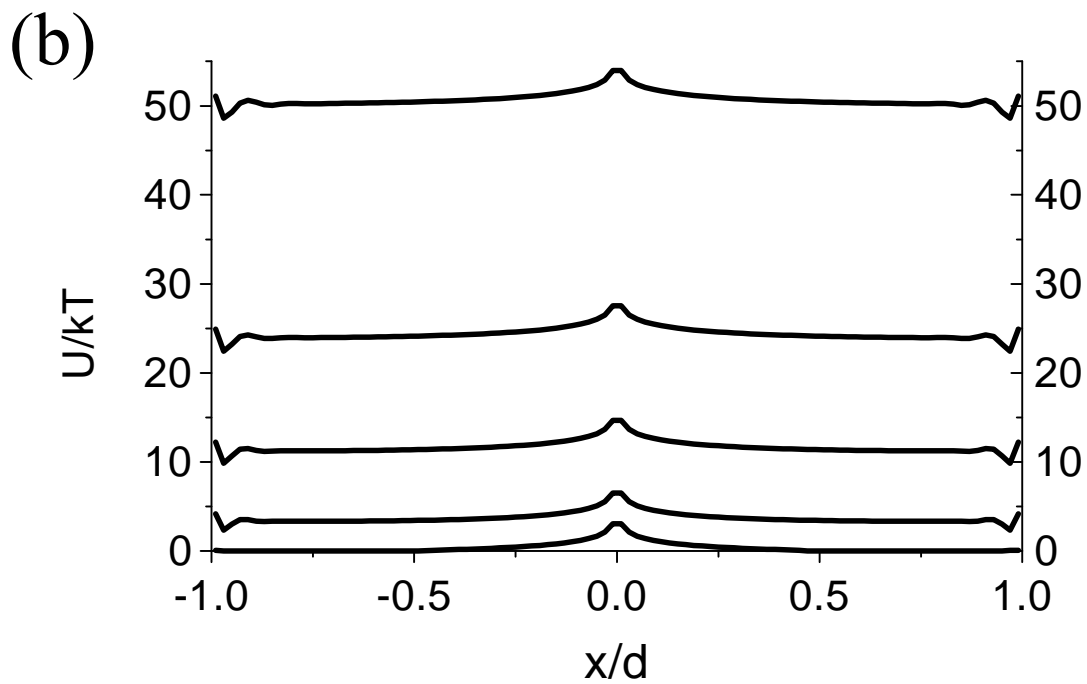
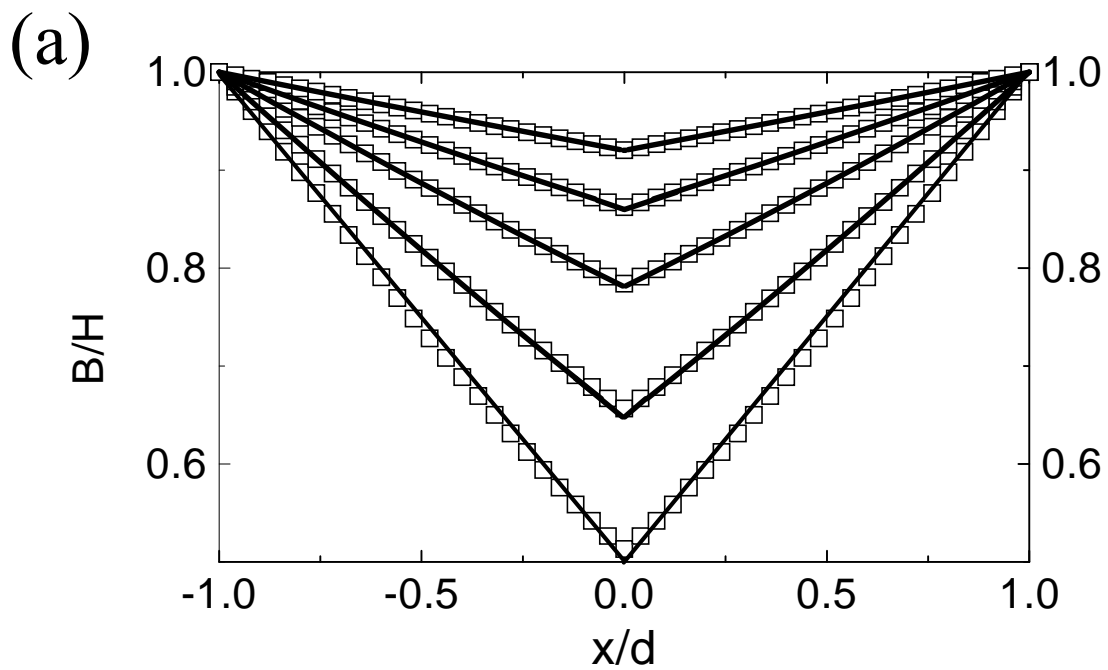
Burlachkov *et al.* Fig.2



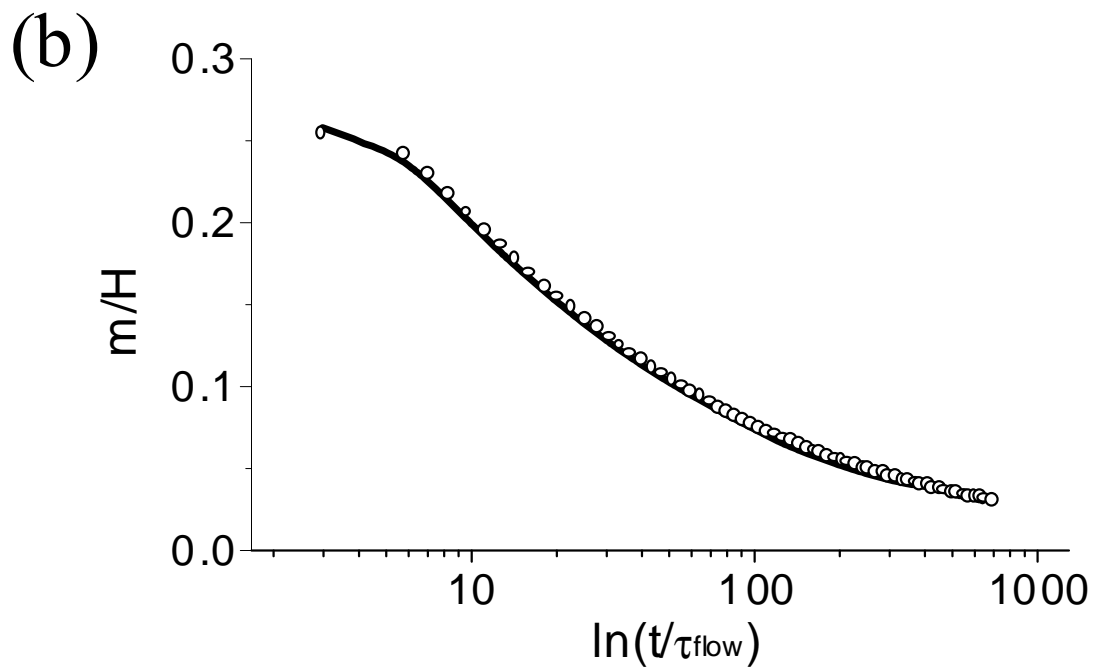
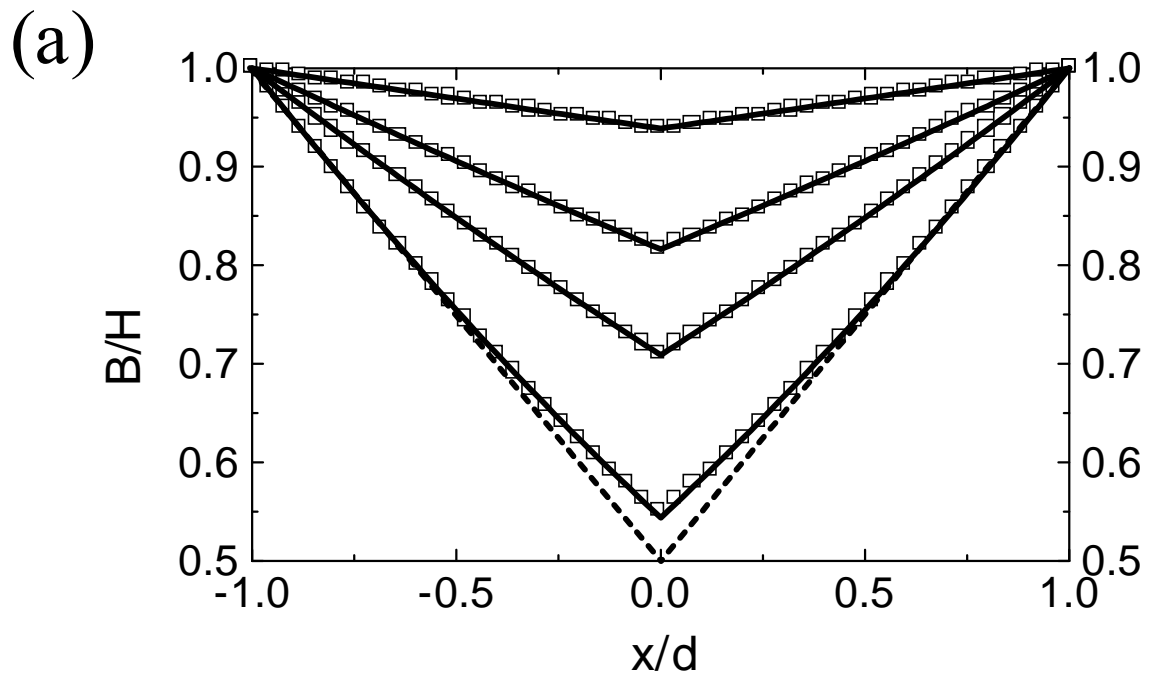
Burlachkov *et al.* Fig. 3



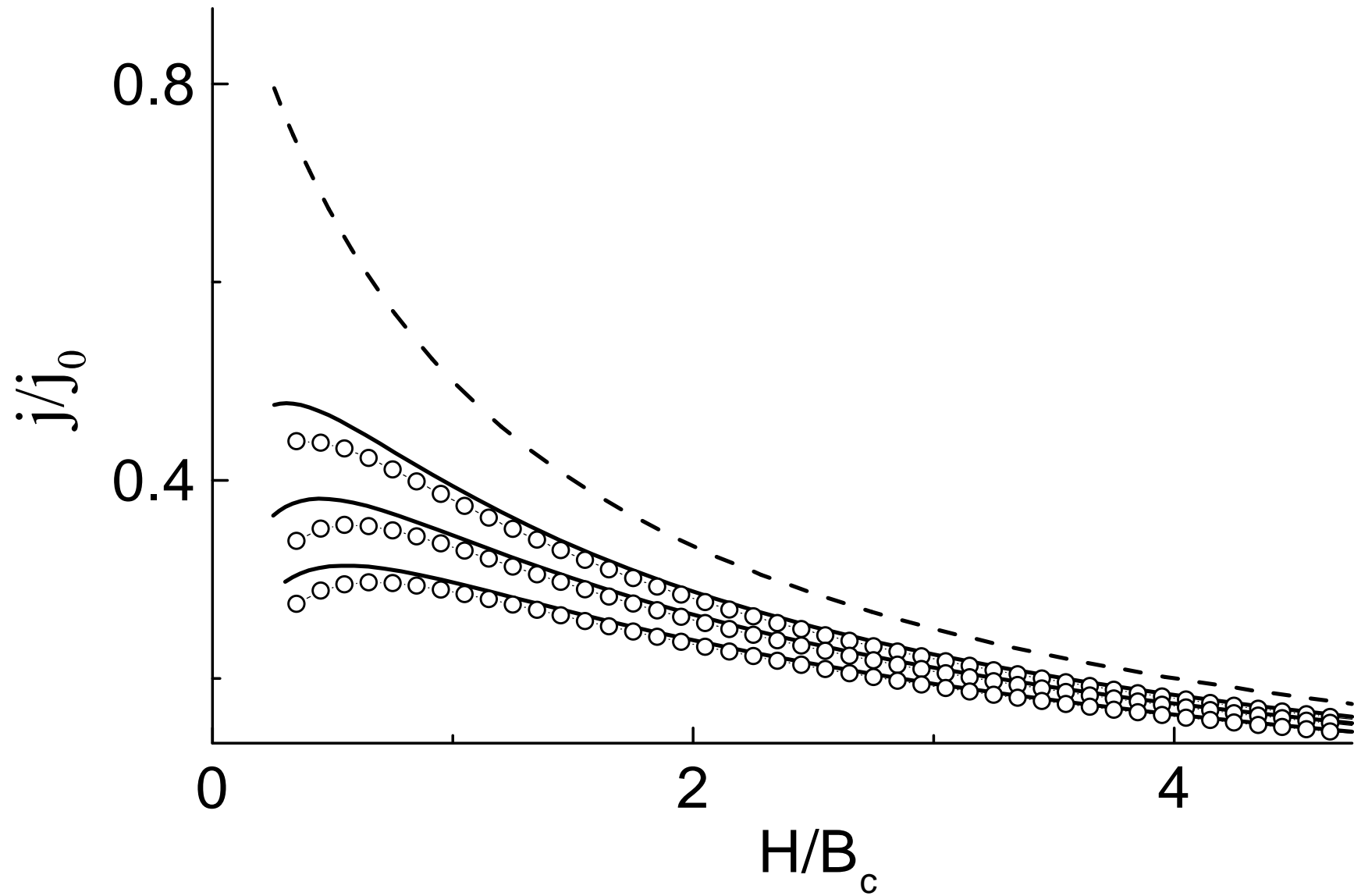
Burlachkov *et al.* Fig.4



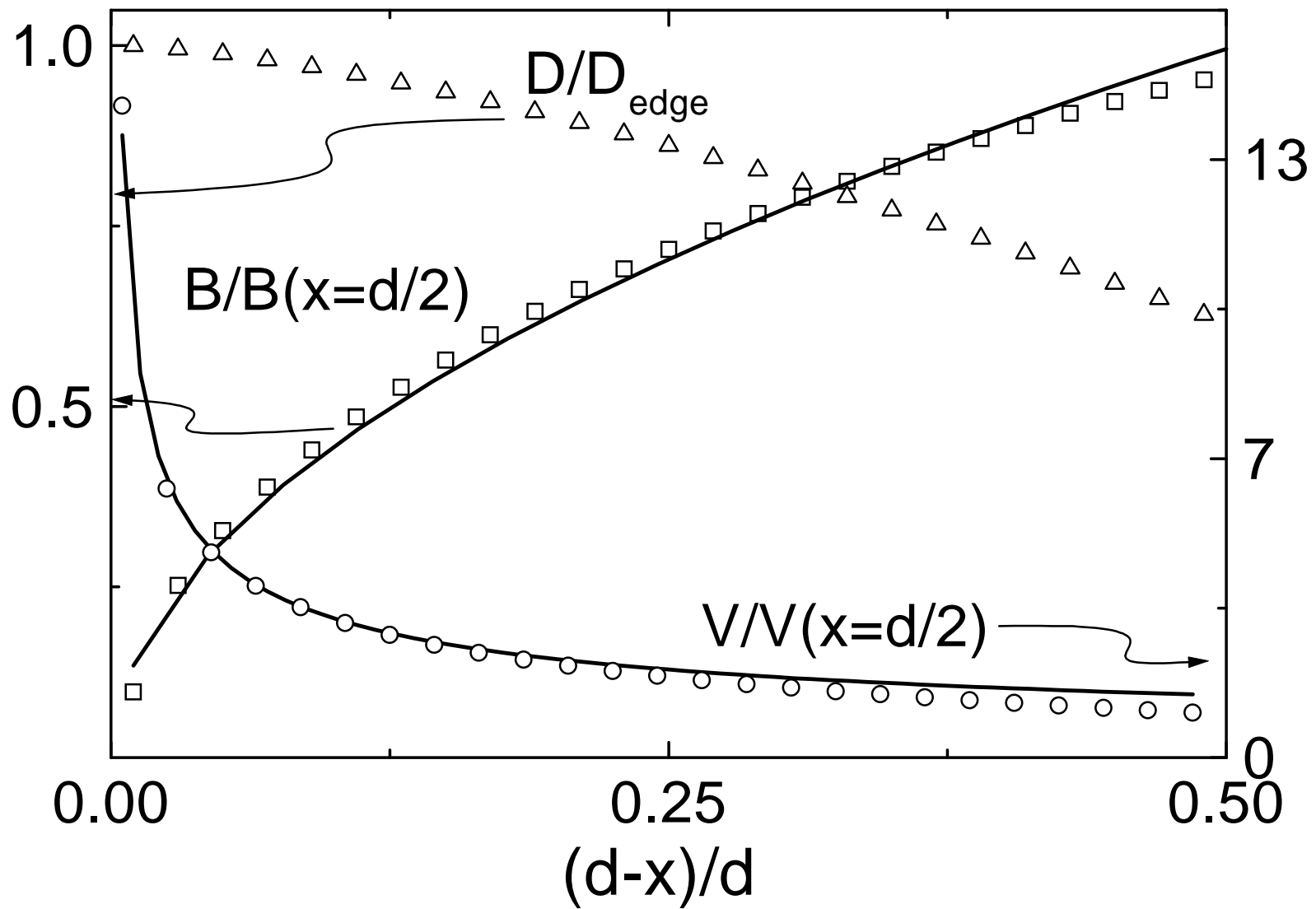
Burlachkov *et al.* Fig. 5



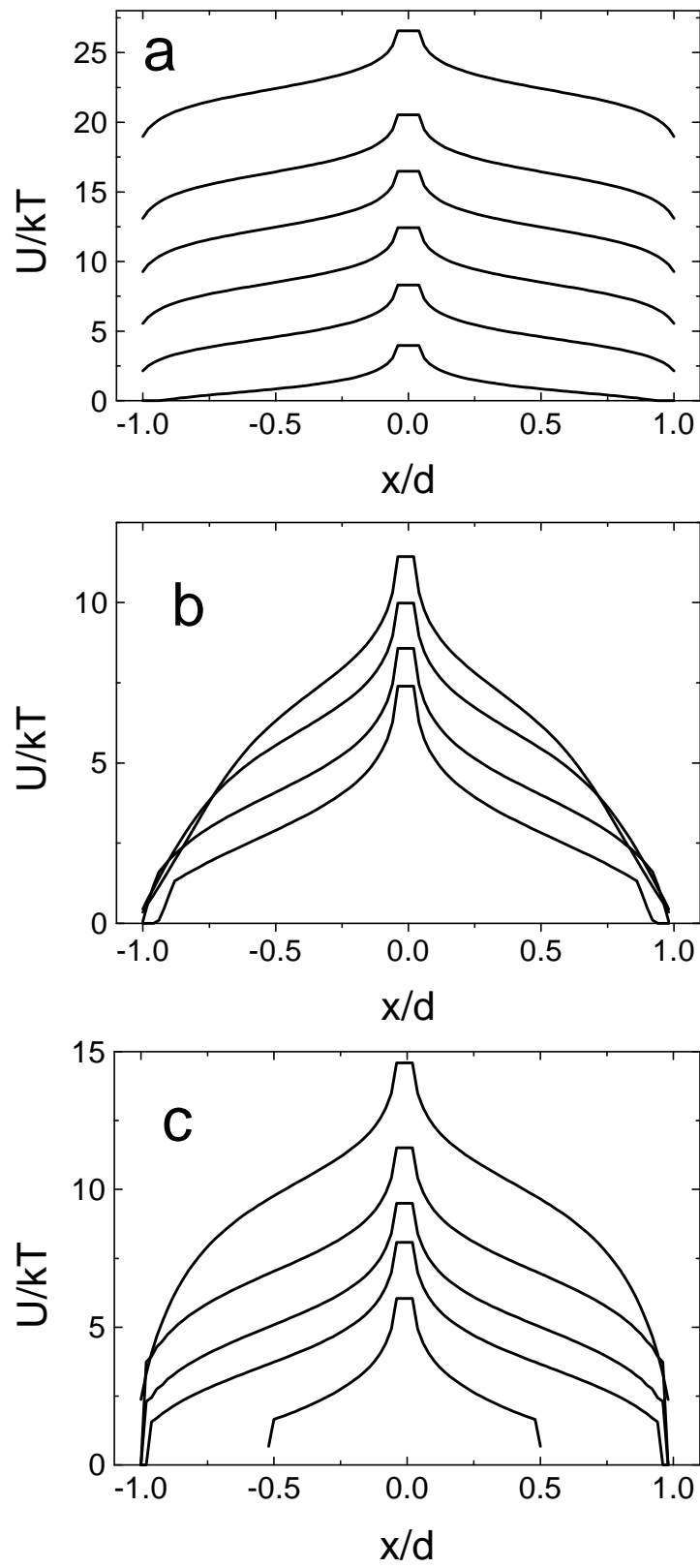
Burlachkov *et al.* Fig. 6



Burlachkov *et al.* Fig. 7



Burlachkov *et al.* Fig. 8



Burlachkov *et al.* Fig.9